

1 **Abstract:**

2 Nowadays, the condition-based maintenance (CBM), in which repairs are triggered by the heuristic symptoms
3 of the component faults, is finding increasing applications in the industrial fields. However, for the high-
4 precision machine tools, the conventional CBM might not be the optimal option, which is uneconomic and
5 incapable of ensuring their machining accuracy. In order to overcome these shortcomings, this paper propose
6 the manufacturing-error-based maintenance (MEBM), where the repairs are initiated based on the
7 manufacturing errors instead of the heuristic symptoms. In MEBM, repairs are taken properly at the occurrence
8 of the excessive machining errors, and therefore, the premature and redundant maintenance can be avoided
9 and the maintenance cost can be minimized; what's more, the machining errors are controlled in the closed
10 loops, and therefore, the machining accuracy can be guaranteed. Based on the principles of the MEBM, a
11 prototype maintenance system – the transient backlash error (TBE) based maintenance system – is established.
12 To achieve this aim, first, the width of the backlash in the mechanical chain is measured by utilizing the built-
13 in encoders and the analytical mapping relationship between the backlash width and the TBE is derived.
14 Relying on these foundations, the TBE can be indirectly estimated. Then, the warning threshold of the TBE is
15 customized according to the permissible roundness error of the workpiece. Thus, the maintenance actions can
16 be precisely implemented: when the monitored TBE exceeds its warning threshold, maintenance workers will
17 be notified to lessen the backlash width, and meanwhile, the permissible maximal size for the backlash will
18 also be informed.

19

20 *Keywords:* CNC machine tools; Machining error; Maintenance; Mechanical chain accuracy; Lead error;
21 Backlash.

1. Introduction

Maintenance has become increasingly important and versatile in industrial field. For critical and fatal systems, such as aircrafts, submarines, and nuclear systems, preventative and predictive maintenance has been widely adopted to reduce the sudden stoppages, thus, to achieve the reliability capabilities of the equipment and to minimize the catastrophic disasters [1]. For equipment manufacturers, condition monitoring systems can provide them with valuable feedback for constant improvement of their equipment [2]. For production systems (e.g. machine tools), proper maintenance contributes positively to product quality enhancement, production increment, and life-cycle cost reduction [3-4].

Historically, breakdowns were considered as random occurrences [5-6]. Only when the equipment ceased to work, was it repaired to prolong its life span. After the 1950s, it was discovered that the failure times are actually distributed in a certain way rather than completely intangibly. Since then, the concept of preventative maintenance (PM) has been advocated, and time-based maintenance (TBM) has been intensively studied relying on the priori knowledge of failure time distribution (FTD) or the degradation model [4, 7-8]. The main ambition of the TBM is to reduce or even eliminate the sudden breakdowns. This is because compared with the scheduled PM, the sudden breakdowns generally require more maintenance cost (time), and in some cases, it might lead to catastrophic disasters. Unfortunately, in industrial fields, it is always quite difficult or even impossible to derive the exact FTD or the degradation model, which has prohibited the feasibility and widespread use of the TBM [2].

Since the 1970s, due to the theoretical development in signal processing and pattern recognition techniques, researchers have achieved remarkable success in the technology of mechanical fault diagnosis [7, 9]. Thereafter, the condition-based maintenance (CBM) was put forward, where the predictive repairs are taken when symptoms of the component faults are detected. If there is a proper diagnostic technique, CBM is capable of getting rid of the failures timely, and therefore, is particularly beneficial to maintain the reliability capabilities of the critical equipment.

Apart from the critical systems, CBM has also been widely applied in production systems (e.g. the machine tools). In [10], Tsai et al. proposed a technique that can detect the onset of preload loss in a ball screw via monitoring the change of the ball pass frequency. Then, when the onset of preload loss is identified, repairs would be initiated and carried out on the ball screw. In [11], several characteristic parameters (e.g. positioning error and reversal error) were extracted from the built-in encoders, and then transferred to the frequency

1 domain that can be interpreted as the order spectrum of these parameters. Experimental results show that
2 deterioration of the feed drive caused by wear can raise the amplitude of these parameters and their spectrums.
3 In [12], Park et al. adopted statistical analysis techniques to detect the anomaly of the monitored data series
4 (namely the injection molding process parameters); and when the abnormal trend is found, maintenance
5 information would be notified to maintenance workers. In addition, by adopting different signals, like the
6 vibration, acoustic emission (AE) and surface roughness, various condition monitoring techniques have been
7 proposed for diagnosing the defects in the spindle bearings [13-14].

8 From these aforementioned examples, it can be found that the reliability-centred CBM, originally proposed
9 for the critical systems, is also beneficial to improve the reliability and production quality of the production
10 system: timely maintenance actions are generally taken once the heuristic symptoms for incipient faults are
11 detected. However, for the high-precision machine tools, the conventional CBM might not be the optimal
12 option because of the following two reasons.

13 (1) For the high-precision machine tools, cost-effectiveness and manufacturing accuracy are their most vital
14 performance indicators, and the weak defects as well as the sudden breakdowns are generally allowable [15].
15 Therefore, the machine tools can actually be utilized as long as they can provide the required machining
16 accuracy. Hence, if the CBM is applied, the machine tools might experience excessively proactive and
17 redundant maintenance, and consequently, substantial maintenance cost can be resulted in.

18 (2) In most of the CBM cases, only the condition of the critical component was monitored and qualitatively
19 evaluated by some indicators, and there was always a lack of mapping procedure from the component condition
20 indicators to the machining accuracy. This means that the machining accuracy is actually unbeknown, and
21 therefore, cannot be properly ensured.

22 Therefore, in this paper, we endeavour to propose a new maintenance strategy, the manufacturing-error-
23 based maintenance (MEBM) system, where the real-time manufacturing errors of the machine tools are
24 monitored as the feedback of the maintenance system and the input of the maintenance system is specified
25 according to the required machining accuracy. When the monitored machining error exceeds the permissible
26 machining error, the maintenance action will be triggered. The ambition of this new maintenance strategy is
27 to reduce the maintenance cost as much as possible, and moreover, to realize the closed-loop control of the
28 machining accuracy.

1 In order to clearly present this newly proposed maintenance strategy to readers, this paper is organized as
2 follows. Section 2 gives a general introduction of the MEBM, including its concept, advantages, as well as the
3 potential key research points. Then, based on the principles of MEBM, a prototype MEBM system – the
4 transient backlash error (TBE) based maintenance system – is established step by step in Sections 3-5. In detail,
5 Section 3 puts forward approaches for characterizing the accuracy of the feed drive mechanical chain by using
6 the built-in encoder signals, and thereafter, the deterioration mechanism of the mechanical chain accuracy is
7 investigated. In Section 4, the manufacturing errors caused by the mechanical chain inaccuracy are discussed,
8 aiming to prove that in the full-closed loop CNC machine tools, the TBE (the contour error caused by the
9 backlash) is the most crucial one, and therefore, worth monitoring and controlling. Subsequently, the mapping
10 relationship between the backlash width (an indicator for specifying the mechanical chain accuracy) and the
11 TBE is analytically derived. Based on the results given in Sections 3 and 4, the TBE can be indirectly estimated.
12 Ultimately, Section 5 fully completes the establishment of the TBE-based maintenance. Conclusions are drawn
13 in Section 6.

14 **2. Framework of the manufacturing-error-based maintenance**

15 **2.1 Outline of the MEBM**

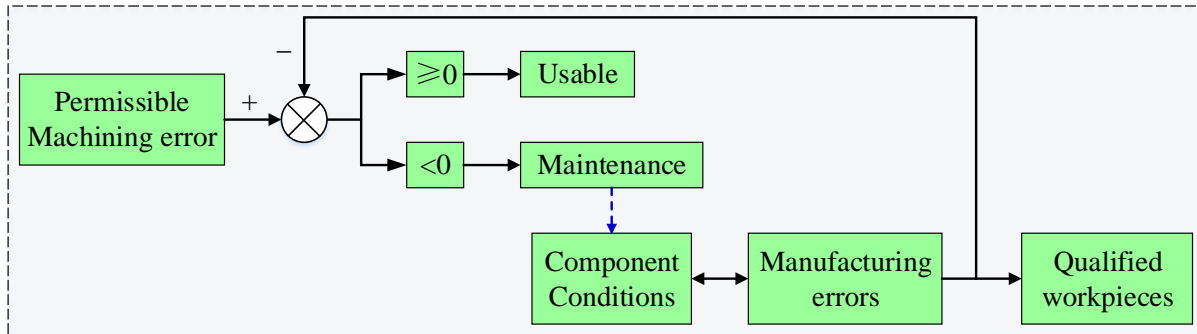
16 The system block diagram of the MEBM is exhibited in Fig. 1. It can be found that the MEBM resembles
17 a closed-loop control system, where the input of the maintenance system is the permissible machining error,
18 the real-time machining error of the machine tool is monitored as the feedback. When the monitored machining
19 error exceeds the permissible machining error, maintenance actions are initiated. With the aid of the closed-
20 loop control, the machining accuracy can be guaranteed; besides, since the repairs will be taken properly at the
21 occurrence of excessive machining errors, the premature and redundant repairs can be avoided and
22 maintenance cost can be minimized.

23 It can be found that to construct the MEBM, the machining errors must be monitored in real time. There
24 are mainly two ways to determine the machining errors: indirect estimation and direct measurement.

25 (a) Indirect estimation: when the mapping relationship between the component condition and the machining
26 error has been derived, the machining error can be indirectly estimated from the condition of the component.
27 What's more, under such situation, the related component is apparent and its satisfactory condition level can
28 be inversely determined from the permissible machining error.

1 (b) Direct measurement: when the mapping relationship between the machining error and its error source
 2 is unbeknown, the machining error must be directly measured. In these cases, additional diagnosis techniques
 3 are required to locate the related components. Of course, when the mapping relationship between the
 4 component condition and the machining error is already known, direct measurement is also feasible.

5 It can be found that it is quite beneficial to develop the mapping relationship between component condition
 6 and the machining error. First, it enables the indirect estimation of the machining error. Second, the related
 7 component as well as its satisfactory condition level can be precisely determined inversely.



9 Fig. 1 The system block diagram of the MEBM

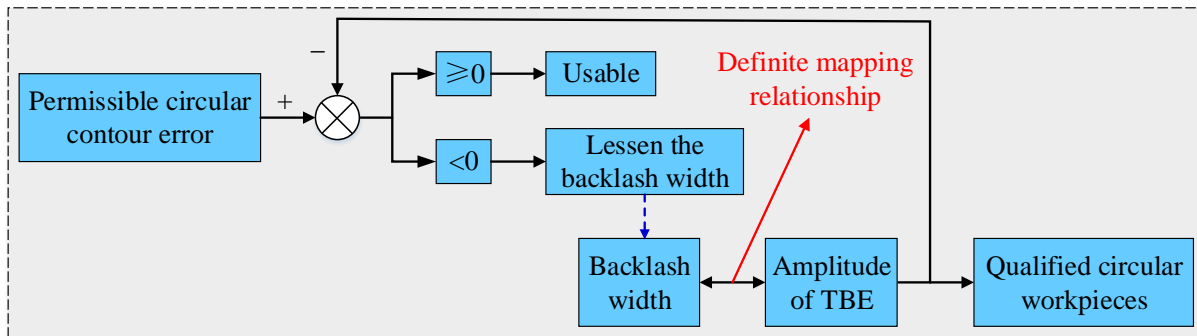
10 2.2 Two typical examples of the MEBM

11 2.2.1 The TBE-based maintenance

12 In [10], Tsai et al. employed the method of Angular Velocity Vold-Kalman Filtering Oder Tracking (AV
 13 VKF-OT) to determine the ball pass frequency of the ball screw in the feed drive. Then, the preload loss of the
 14 ball screw can be diagnosed by detecting the change of the ball pass frequency. Ultimately, once the onset of
 15 preload loss is found, maintenance action is implemented. As we all know, the purpose of preloading the ball
 16 screw is to reduce the clearance (the backlash) as well as the resultant machining error, and thus, to guarantee
 17 the machining accuracy. However, when the preload has just been lost, the resultant machining error is actually
 18 no bigger than the permissible machining error. This implies that it is too early to implement the maintenance
 19 at the onset of the preload loss.

20 Based on the concept of MEBM, the TBE-based maintenance system can be developed as shown in Fig. 2,
 21 where the machining error caused by backlash (e.g. the TBE) is monitored, and then, compared with
 22 permissible machining error. When the amplitude of the TBE is larger than permissible machining error, repair
 23 is carried out on the feed drive mechanical chain to lessen the backlash width. In [16], the mapping relationship
 24 between the backlash width and the TBE is fully defined. Therefore, the TBE can be indirectly estimated from
 25 the backlash width while the backlash width should be measured first.

1 It can be found that compared with the conventional CBM in [10], the TBE-based maintenance system is
 2 capable of not only controlling the TBE in closed loop, but also minimizing the maintenance cost by avoiding
 3 the premature repairs.



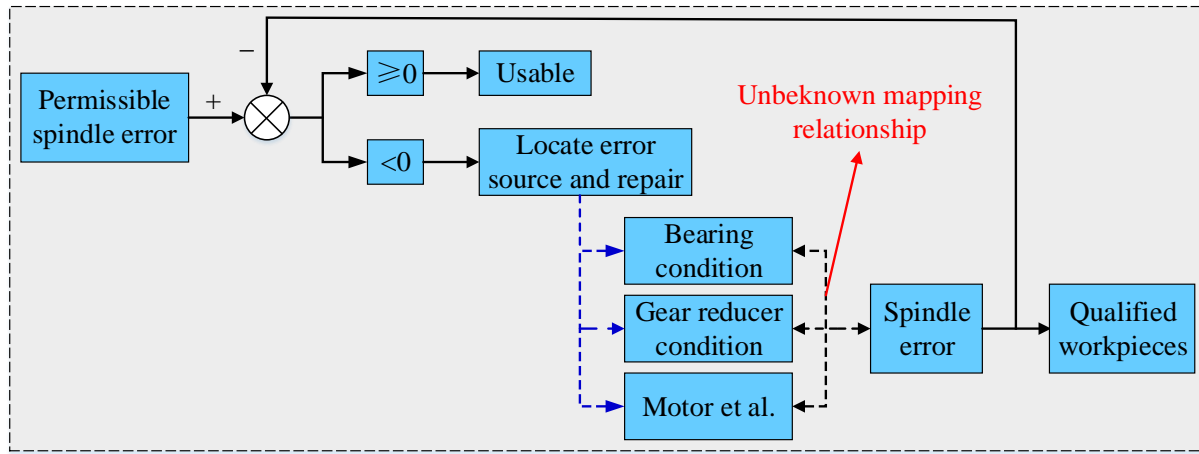
5 Fig. 2 The system block diagram of the TBE-based maintenance

6 2.2.2 The spindle-error-based maintenance

7 Much attention has been paid on diagnosis techniques for seeking the fault signs of the bearings that are
 8 critical components in the spindle subsystem. Up to now, various powerful methods have been proposed, for
 9 example, the time and frequency domain analysis [13-14], the wavelet denoising [17], the spectral kurtosis
 10 (SK), and the minimum entropy deconvolution (MED) [18]. However, unlike the diagnosis techniques, the
 11 mapping relationship between the condition of the bearing and the performance of the spindle subsystem (e.g.
 12 the spindle error) has rarely be researched. In other words, in the conventional CBM, the spindle error wasn't
 13 estimated, and therefore, couldn't be guaranteed easily. In practice, for guaranteeing the precision of the
 14 spindle, repairs are generally carried out once the signs of bearing defects are detected. As a consequence, the
 15 spindle subsystem experiences extremely redundant maintenance, which takes immense expense.

16 Based on the concept of MEBM, the spindle-error-based maintenance system can be developed as shown
 17 in Fig. 3. Unfortunately, since the mapping relationship between the spindle error and its error sources remains
 18 enigmatic, the spindle error could only be determined by direct measurement while indirect estimation is
 19 infeasible; what's worse, before implementing the maintenance, additional diagnostic analysis is still required
 20 for locating the error sources. The approaches for measuring the spindle error can be found in [19-20].

1



2

Fig. 3 The system block diagram of the spindle-error-based maintenance

2.3 Key research points for the MEBM

From the discussion given above, it can be found that the newly proposed MEBM is initiated based on the machining errors instead of the heuristic symptoms of the component defects. Therefore, the MEBM is not only capable of controlling the machining accuracy by adopting the closed machining-error-control loops, but also helpful to minimize maintenance cost by avoiding the premature and redundant maintenance.

However, in order to apply the MEBM strategy to machine tools, more attention still should be paid to the following research points.

(1) Development of the mapping relationship between component condition and the machining error. Section 2.1 shows that on one hand, it enables the indirect estimation of the machining error; on the other hand, the related component as well as its satisfactory condition level can be precisely determined inversely.

(2) Measurement of the component condition. Apart from the mapping relationship, in order to realize the indirect estimation of the machining error, the component condition should also be measured in advance.

(3) Identification of the crucial machining errors. Ideally, for guaranteeing the machining accuracy of machine tools, all of the machining errors should be monitored and controlled in closed loops. However, this might result in a huge and costly monitoring system. Hence, to improve the feasibility and economy of the MEBM strategy, the critical machining errors should be identified and paid more attention. In this paper, the crucial machining errors refer to these that contribute most to the overall machining error and suffer severe deterioration.

Based on the principle of MEBM, the construction method of TBE-based maintenance will be elaborated step by step in the Sections 3-5.

3. Measurement of mechanical chain accuracy and its deterioration mechanism

In order to construct the TBE-based maintenance, the backlash width should be measured first. By utilizing the built-in encoders, this section will propose a method to evaluate the accuracy of the feed drive mechanical chain, including the measurement of the backlash width and the lead error. The proposed method will only be feasible for the full-closed-loop feed drives, where the position of the sliding table is directly measured by a linear encoder to provide the position feedback while the rotating speed of the servomotor is picked up by a rotary encoder and used as the speed feedback.

Fig. 4 shows the mechanical structure of Y-axis, on a vertical machining centre. It can be found that Y-axis is a closed-loop feed drive. Its specifications are shown in Table 1. Unless otherwise stated all the experiments will be conducted on this feed drive.

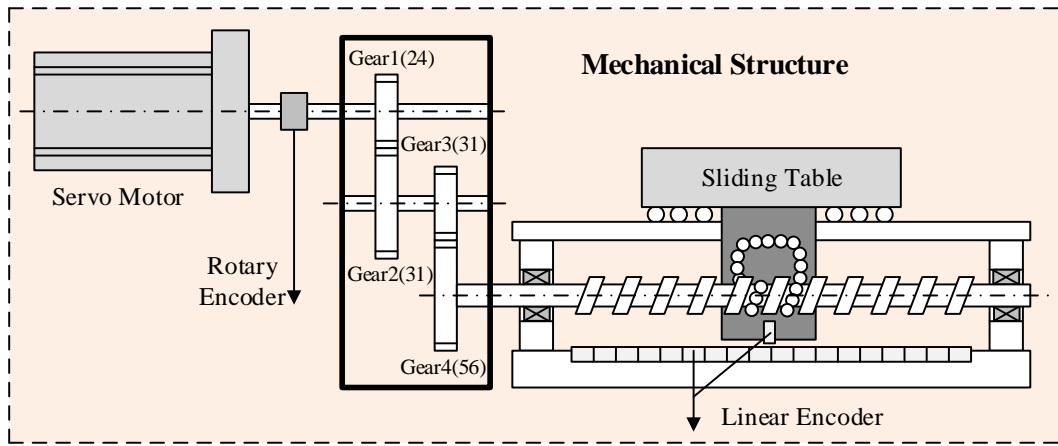


Fig. 4 The mechanical structure of Y-axis

Table 1 Specifications of the mechanical chain in Y-axis

Item	Value
Teeth number for Gear #1	24
Teeth number for Gear #2	31
Teeth number for Gear #3	31
Teeth number for Gear #4	56
Nominal screw pitch	16 mm/rev.
Transmission ratio k_a	6.857 mm/rev
Length of the useful travel	1000 mm

3.1 Lead error

3.1.1 Measurement of the lead error

1 The lead error is the most commonly used index for characterizing the accuracy of the ball screw. In ISO
 2 3408-3:2006, four criteria are defined for specifying the lead error of the ball screw [21]. In this paper, these
 3 four criteria will be utilized to specify the lead error of the mechanical chain that consists of not only the ball
 4 screw, but also a two-stage gearbox.

5 (1) Actual mean travel deviation e_p : the difference between the actual mean travel l_m and the nominal
 6 travel l_0 over the full useful travel, as indicated by the blue dimension annotation on the right side. Here, l_0
 7 represents the nominal travel of the sliding table that can be given by the product of the servomotor travel x_m
 8 and the transmission ratio k_a ; l_a refers to the actual travel of the sliding table x_l ; and the actual mean travel
 9 l_m indicates the straight line that has the best fit to l_a . In Fig. 5, the black solid line represents the actual travel
 10 l_a , the blue solid line means the actual mean travel l_m , and the red solid line indicates the nominal travel l_0
 11 that is also used as the reference coordinate (independent variable) of these three lines.

12 Please note that for a clearer exhibition, when drawing Fig. 5, l_0 has been subtracted from the three
 13 dependent variables l_a , l_m , and l_0 . That's why the nominal travel l_0 keeps at *zero* over the whole travel, and
 14 the vertical axis of the graph is labelled 'Travel deviation'.

15 (2) Travel variation v_u : the band width (i.e. the range) of the travel variation over the whole useful travel,
 16 as indicated by the two green dotted lines in Fig. 5. Here, the travel variation means the deviation between the
 17 actual travel l_a and the actual mean travel l_m , written as $(l_a - l_m)$. It can be found that $(l_a - l_m)$, over the
 18 whole useful travel, is bordered by the two green dotted lines which are parallel to l_m . The distance between
 19 the two straight lines equals v_u . Mathematically, v_u can also be given by

$$20 \quad v_u = [\max(l_a - l_m) - \min(l_a - l_m)]_{|useful\ travel} \quad (1)$$

21 (3) Travel variation v_{300} : the maximum band width of $(l_a - l_m)$ for any 300 mm travel over the whole
 22 useful travel, as indicated by the two dashed red lines on Fig. 5. v_{300} is given by

$$23 \quad v_{300} = \max\{[\max(l_a - l_m) - \min(l_a - l_m)]_{|300mm\ travel}\}_{|useful\ travel} \quad (2)$$

24 (4) Travel variation $v_{2\pi}$: the maximum band width of $(l_a - l_m)$ within any pitch travel over the full useful
 25 travel, as indicated by the two pink dot dash lines on the partial enlarged view of Fig. 5. $v_{2\pi}$ can be written as

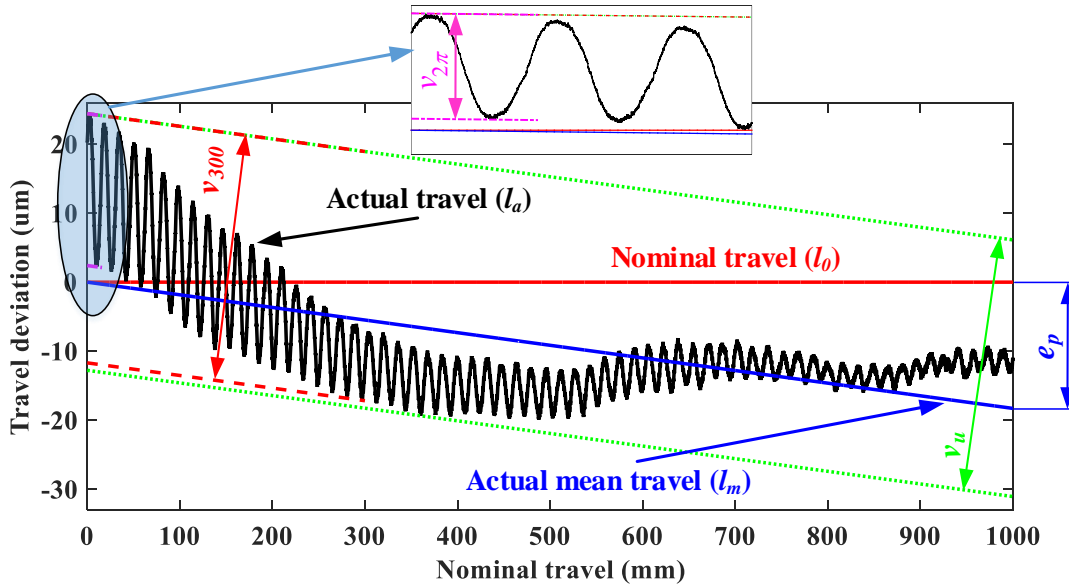
$$26 \quad v_{2\pi} = \max\{[\max(l_a - l_m) - \min(l_a - l_m)]_{|2\pi\ travel}\}_{|useful\ travel} \quad (3)$$

27 In the full-closed-loop feed drives, when the feed drive is programmed to take a one-way travel, the
 28 servomotor travel x_m can be measured by the rotary encoder mounted on the motor shaft, and synchronously,

1 the actual travel of the sliding table x_l can be measured via the linear encoder. Thus, the nominal travel l_0 can
 2 be derived by $k_a x_m$ and the actual travel l_a just equals x_m . Based on the two travels l_0 and l_a , the four criteria
 3 e_p , v_u , v_{300} , and $v_{2\pi}$ can ultimately be derived for characterizing the lead error.

4 Fig. 5 shows the measurement results of the lead error in Y-axis on 2013-07-13. The four criteria were
 5 $e_p = -18.29 \mu\text{m}/1000\text{mm}$, $v_u = 37.18 \mu\text{m}$, $v_{300} = 36.10 \mu\text{m}$, and $v_{2\pi} = 22.00 \mu\text{m}$, respectively.

6



7 Fig. 5 The lead error of the mechanical chain in Y-axis on 2013-7-13

8 3.1.2 Deterioration law of the lead error

9 To figure out the degradation law of the lead error in Y-axis, a long period of tracking measurement was
 10 conducted. During the whole period, the machining centre was used as usual in an ordinary workshop without
 11 the temperature control system. The utility time d and the ambient temperature t of each measurement are
 12 shown in Table 2.

13 Table 2 Utility time d and ambient temperature t of each measurement

Measurement No.	1	2	3	4	5	6	7	8	9
Utility time d (day)	0	9	26	36	58	85	118	180	215
Temperature t ($^{\circ}\text{C}$)	7	9	5	9	15	21	23	19	10

14

15 The mean travel deviation e_p and the ambient temperature t are displayed on Fig. 6; and the travel variations

16 v_u , v_{300} , $v_{2\pi}$ as well as t are displayed on Fig. 7.

1

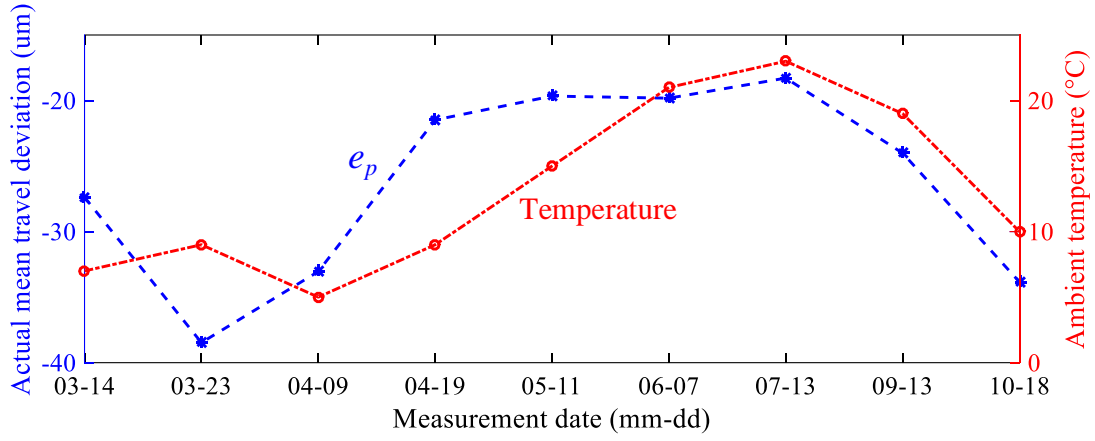


Fig. 6 Deterioration law of the actual mean travel deviations e_p

2

3

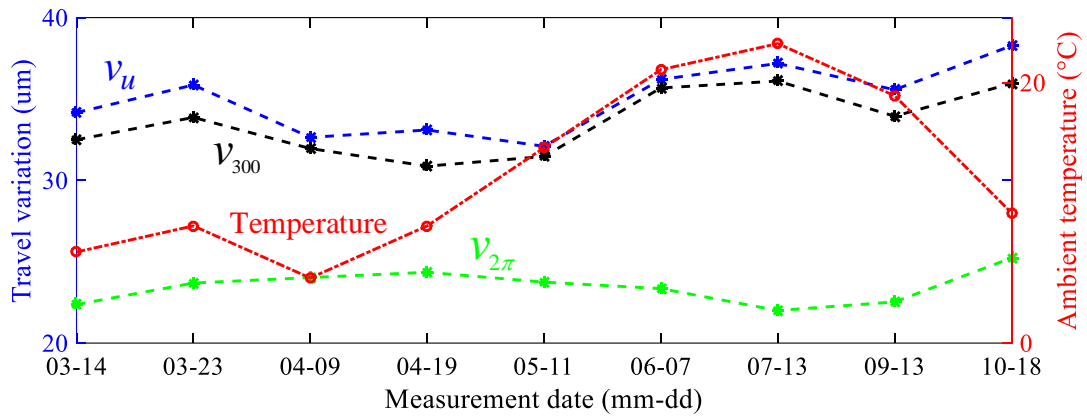


Fig. 7 Deterioration mechanism of the travel variations v_u , v_{300} , and $v_{2\pi}$

4

5 From Fig. 6, it can be found that during the tracking experiments, the actual mean travel deviation e_p has
 6 changed severely, from $-38.47 \mu\text{m}/1000\text{mm}$ to $-18.29 \mu\text{m}/1000\text{mm}$, indicating that the resultant
 7 machining error might also vary significantly. Therefore, the machining error caused by e_p may need
 8 monitoring.

9 Fig. 7 shows that compared with e_p , the changing range of the travel variations v_u , v_{300} , $v_{2\pi}$ are much
 10 smaller: for v_u from $34.17 \mu\text{m}$ to $38.27 \mu\text{m}$, for v_{300} from $32.5 \mu\text{m}$ to $35.96 \mu\text{m}$, and for $v_{2\pi}$ from
 11 $22.00 \mu\text{m}$ to $25.23 \mu\text{m}$. This indicates that the resultant machining errors might also change insignificantly.

12 In Fig. 6 and Fig. 7, it can also be observed that none of the four criteria increased monotonously. To verify
 13 our observation more rigorously, the correlation coefficients between the criteria and the utility time d are
 14 worked out to be $r_{e_p,d} = 0.1125$, $r_{v_u,d} = 0.6683$, $r_{v_{300},d} = 0.6397$, and $r_{v_{2\pi},d} = 0.1337$, respectively. The
 15 tiny correlation coefficients $r_{e_p,d}$ and $r_{v_{2\pi},d}$ mean that the wear plays a negligible role in the change of e_p and

1 $v_{2\pi}$, while the relatively bigger correlation coefficients $r_{v_{u-d}}$ and $r_{v_{300-d}}$ suggest that the deterioration of v_u
 2 and v_{300} is related with the wear.

3 Similarly, the correlation coefficients between the criteria and the ambient temperature t are also worked
 4 out to be $r_{e_p-t} = 0.7044$, $r_{v_{u-t}} = 0.4223$, $r_{v_{300-t}} = 0.5877$, and $r_{v_{2\pi-t}} = -0.5207$, respectively. It can be
 5 found that the actual mean travel deviation e_p is strongly correlated with the ambient temperature t : when the
 6 temperature goes up, the pitch of the ball screw becomes longer.

7 Here, the Pearson product-moment correlation coefficient is adopted, written as

$$8 \quad r_{X-Y} = \frac{\text{cov}(X,Y)}{\sigma_X \sigma_Y} \quad (4)$$

9 where $\text{cov}(X, Y)$ is the covariance of X and Y; and σ_X is the standard deviation of X.

10 **3.2 Backlash width**

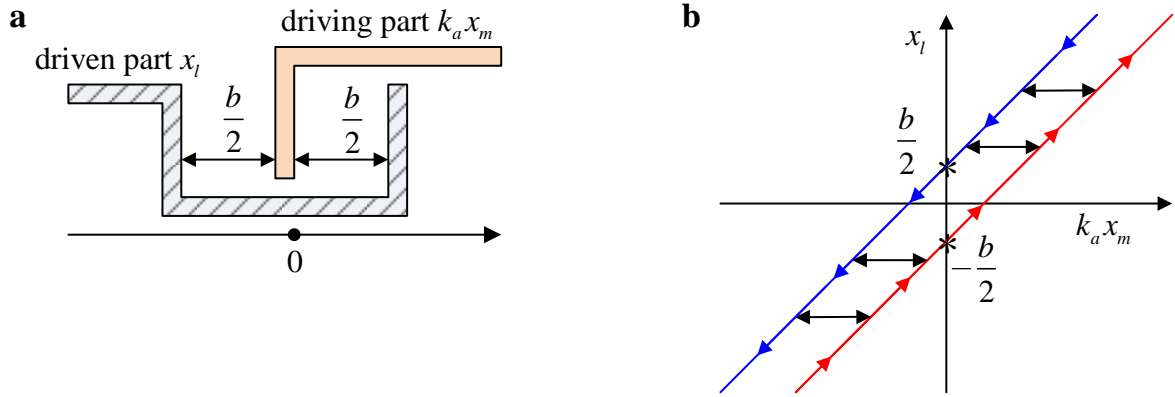
11 3.2.1 Measurement of the backlash width

12 Apart from the lead error, the backlash width is also a critical criterion for specifying the accuracy of the
 13 feed drive mechanical chain. The mechanical chain with backlash can be simplified as the friction-driven
 14 hysteresis model as shown in Fig. 8 (a), where the servomotor as well as the transmission chain is assumed as
 15 the driving part, the sliding table is assumed as the driven part, and the flexibility of the mechanical chain is
 16 not considered. It can be derived that in this model, the motion of the driving part is given by the product of
 17 the servomotor displacement and the transmission ratio $k_a x_m$, the motion of the driven part equals the
 18 displacement of the sliding table x_l , and the size of the total clearance is denoted by b , termed the backlash
 19 width. Based on this model, the dynamic relationship between $k_a x_m$ and x_l can be derived:

$$20 \quad \begin{cases} x_{l+} = k_a x_m - \frac{b}{2} & \text{feeding positively} \\ x_{l-} = k_a x_m + \frac{b}{2} & \text{feeding negatively} \end{cases} \quad (5)$$

21 as shown in Fig. 8 (b).

1



2 Fig. 8 The backlash element: (a) the structure schematic diagram and (b) the dynamic characteristics

3 Eq. (5) and Fig. 8 (b) indicate that when the servomotor arrives at a given position x_m , the sliding table is
 4 possibly at the two different positions: x_{l+} when feeding positively and x_{l-} when feeding negatively. As a
 5 consequence, two separated lines are generated (see Fig. 8 (b)): the upward side $k_a x_m \sim x_{l+}$ as shown by the
 6 red line and the downward side $k_a x_m \sim x_{l-}$ as exhibited by the blue line.

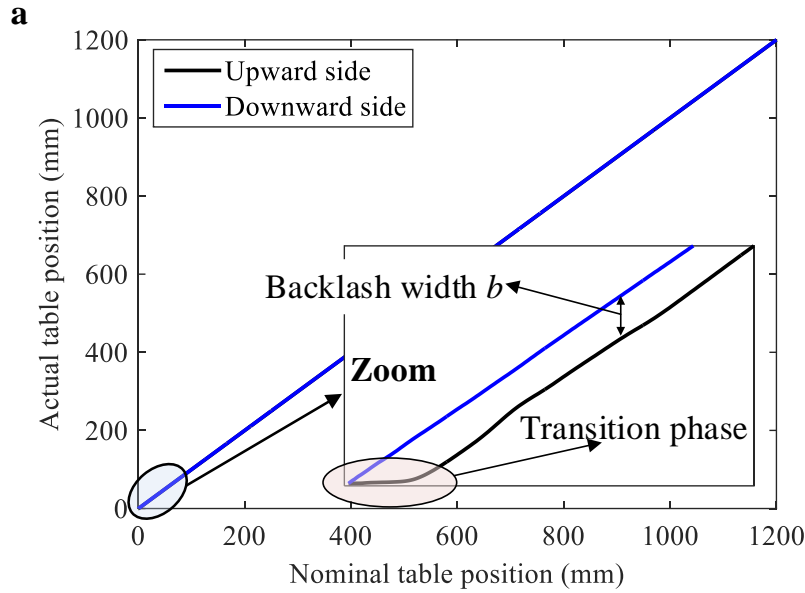
7 Besides, from this model, it can be derived that the backlash width b is equal to vertical distance between
 8 the upward side line and the downward side line, i.e. the difference between x_{l-} and x_{l+} .

9 In the full-closed-loop feed drives, the motor position x_m and the table position x_l could be picked up from
 10 the rotary and the linear encoders, respectively. Therefore, when the axis is programmed to make a round trip
 11 over the measurement travel, the upward side $k_a x_m \sim x_{l+}$ and the downward side $k_a x_m \sim x_{l-}$ can be obtained.
 12 Based on this, the backlash width b can be finally determined.

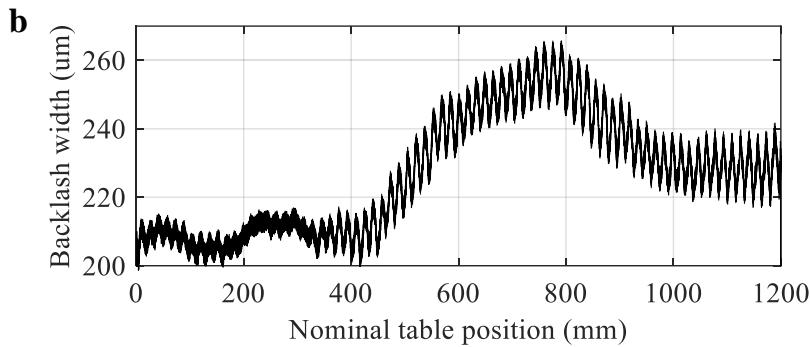
13 Fig. 9 shows the measurement results of backlash width in Y-axis on 2013-07-13. It can be found that the
 14 backlash width is a position-dependent variable.

15

1



2



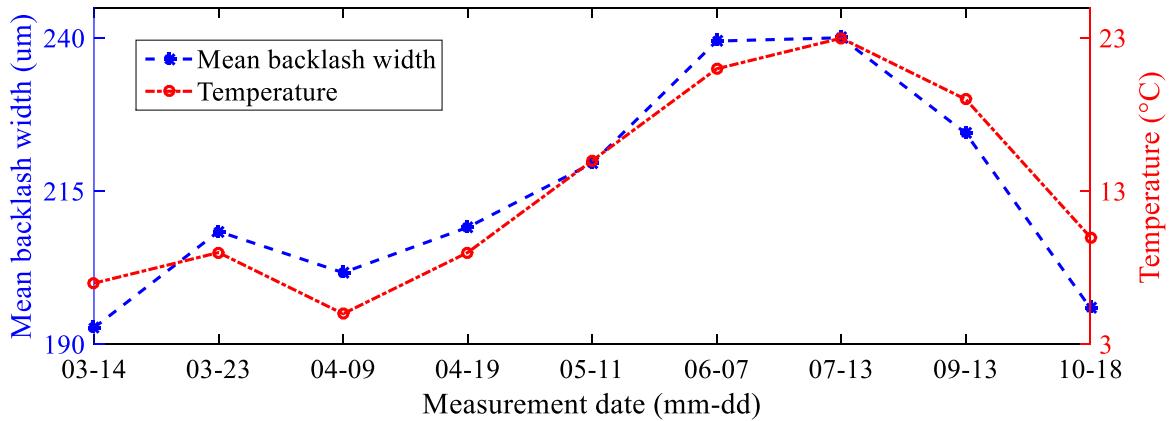
3 Fig. 9 Measurement of the backlash width in Y-axis: (a) the upward side $k_a x_m \sim x_{l+}$ and the downward side
 4 $k_a x_m \sim x_{l-}$ obtained from a round trip, and (b) the backlash width b

5 3.2.2 Deterioration law of the backlash width

6 Similarly, the deterioration law of the backlash width was investigated. The arithmetic means of the
 7 backlash width \bar{b} as well as the ambient temperature t are plotted in Fig. 10. It can be found that during the
 8 long-term measurements, the backlash width changed severely, increased in the early stages and then decreased
 9 from July, which suggests that its resultant machining error might also change significantly, and therefore,
 10 deserve monitoring.

11 The correlation coefficient of the mean backlash width \bar{b} with the utility time d is worked out to be $r_{\bar{b}_d} =$
 12 0.2411, implying that the backlash width hardly deteriorated due to the wear and erosion. Further, the
 13 correlation coefficient between \bar{b} and the ambient temperature t is worked out to be $r_{\bar{b}_t} = 0.9351$, suggesting
 14 that the change of the backlash widths has strong correlation with the temperature variation, similar as the
 15 changing law of e_p . The phenomena could be explained by the thermal expansion theory: when the temperature
 16 increases, both the screw and the balls expands, but the screw expands more significantly than the balls.

1 Consequently, when the temperature goes up, both the actual mean travel deviation e_p and the backlash width
 2 b increase.
 3



4 Fig. 10 Deterioration law of the mean backlash widths \bar{b}

5 In this section, methods are proposed for measuring the mechanical chain accuracy. It can be found that in
 6 the full-closed-loop feed drive, the two built-in encoders are ready for collecting the table and the motor
 7 positions, which will then be used to derive the criteria of the mechanical chain accuracy. Hence, no extra
 8 sensors are required.

9 From the long-term measurement results, it can be obtained that compared with the travel variations v_u ,
 10 v_{300} , and $v_{2\pi}$, the actual mean travel deviation e_p and the backlash width b fluctuated more greatly over time.
 11 Through the correlation analysis, it can be revealed that the changes of e_p and b mainly resulted from the
 12 ambient temperature variation, rather than gradual and irreversible wear and erosion. In practice, the
 13 surrounding environment variations (especially the temperature variation) has often resulted in the
 14 performance degradation of the high-precision instrument.

15 4. Machining errors caused by the mechanical chain inaccuracy in the full-closed- 16 loop CNC machine tools

17 4.1 Identification of the crucial machining errors

18 Section 3 puts forward five indicators (including the backlash width b , the actual mean travel deviation e_p ,
 19 and the three travel variations v_u , v_{300} , $v_{2\pi}$) for specifying the accuracy of the mechanical chain. However, in
 20 the MEBM, the repairs are initiated based on the machining errors rather than the component condition

1 indicators. Therefore, before implementing the MEBM, the indicators for specifying the mechanical chain
2 inaccuracy need to be mapped into the corresponding machining errors of the machine tool.

3 In practice, the natures and amplitudes of the machining errors caused by the identical mechanical chain
4 inaccuracy can be different depending on the types of the machine tools as well as the machining parameters.
5 In semi-closed-loop feed drive, since only a rotary encoder is installed on the shaft of the servomotor for
6 providing both the speed and the position feedback, the mechanical chain inaccuracy can result in positioning
7 errors. This paper mainly focuses on the full-closed-loop CNC machine tools, where the positioning errors are
8 completely eliminated. However, the mechanical chain inaccuracy can still result in the following machining
9 errors:

10 (1) Referring to [16], the backlash can result in the transient backlash error (TBE) at the start or directional
11 reversals, which is the one of the most predominant contour errors in the full-closed-loop CNC machine tools.

12 (2) As far as we know, few articles have been published for investigating the machining errors of the full-
13 closed-loop CNC machine tools caused by the travel variations v_u , v_{300} , $v_{2\pi}$. Fortunately, we have
14 successfully conducted some simulations and experiments on a bi-axis contouring system. The results
15 demonstrate that the travel variations could bring about wavy contour errors to the machined profiles. However,
16 compared with the TBE, their amplitudes are much smaller.

17 (3) The actual mean travel deviation e_p hardly degrades the manufacturing accuracy in the full-closed-loop
18 CNC machine tools.

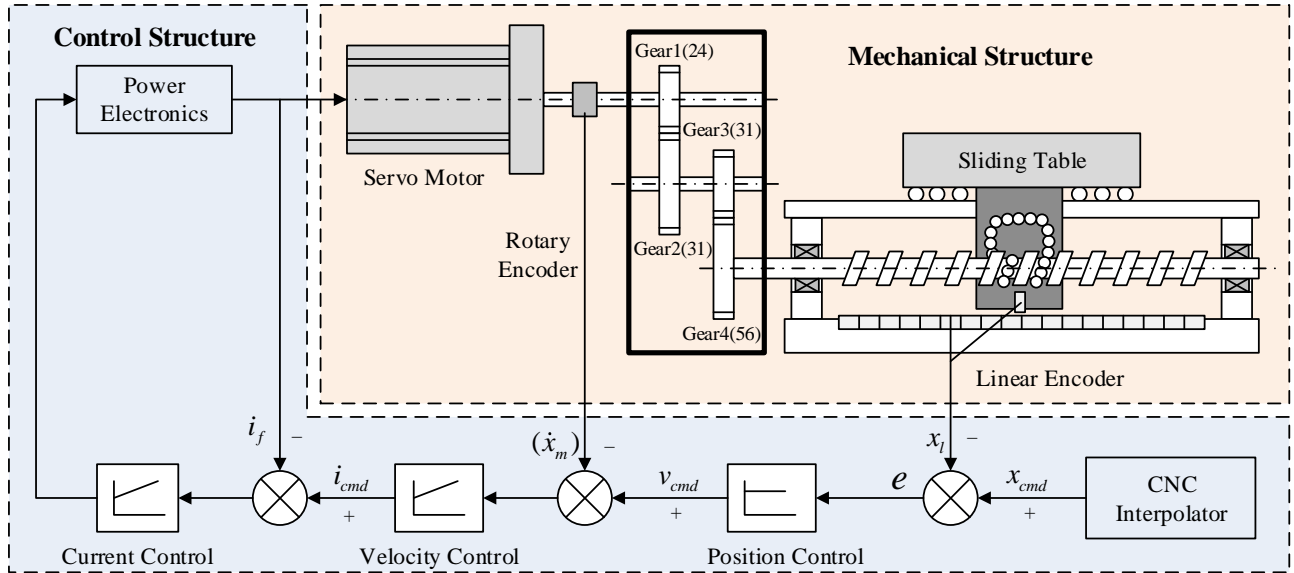
19 Ideally, all the machining errors caused by the mechanical chain inaccuracy should be monitored and
20 controlled in closed loops. However, e_p hardly affects the machining accuracy, and therefore, doesn't deserve
21 the monitoring obviously. Both the backlash and the travel variations can lead to the machining errors. But,
22 the machining error caused by the backlash (i.e. the TBE) is much larger than the machining errors caused by
23 the travel variations. In addition, the long-term measurement results in Section 3 show that the backlash width
24 fluctuated much more severely than the travel variations.

25 Given all that, we can draw the following conclusion: in full-closed loop CNC machine tools, among all the
26 machining errors caused by the mechanical chain inaccuracy, the TBE is the most crucial one, and worth of
27 monitoring and controlling.

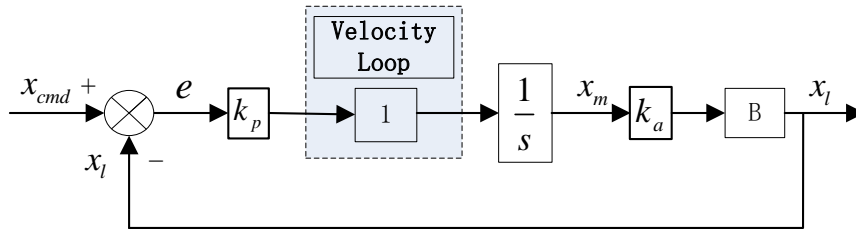
28 In [16], the mechanism and as well as the formulations of the TBE was investigated thoroughly, that will be
29 reviewed briefly in Section 4.2.

1 **4.2 Review of the mapping relationship between the backlash width and the TBE**

2 Fig. 11 exhibits the architecture of Y-axis. It can be found that Y-axis consists of three independent control
 3 loops: the position-control loop, the velocity-control loop, and the current-control loop. Since the two inner
 4 loops (the current-control loop and the velocity-control loops) generally respond much faster than the outer
 5 loop (the position-control loop), the two inner loops can be idealized as units. In this way, a simplified model
 6 for Y-axis could be derived as shown in Fig. 12, where B represents the hysteresis model of backlash.



8 Fig. 11 Architecture of the full-closed-loop Y-axis



10 Fig. 12 Block diagram of the simplified model for Y-axis

11 Owing to the employment of the full-closed-loop control, the positioning errors are completely eliminated.
 12 However, when feeding direction reverses, the backlash in the mechanical chain can still postpone the motion
 13 of the sliding table until the backlash is completely traversed. Based on the simplified model in Fig. 12, the
 14 process of backlash traverse could be described by an integral function

15
$$\int_0^T k_p k_a e d\tau = b \tag{6}$$

16 By solving Eq. (6), the delay time T caused by backlash b could be worked out.

17 If several axes are employed to move synchronously to sculpture a profile, the motion delay caused by
 18 backlash can lead to the incoordination between axes, and consequently, the TBE. Here, we assume that a

1 straight line is milled by a bi-axis (X-axis and Y-axis) contouring system, and at the beginning, the backlash
 2 in Y-axis is directly engaged, and reversely engaged in X-axis. Under such assumption, TBE will emerge at
 3 the initial phase as shown in Fig. 13 (a). Based on the simplified model, the analytical amplitude of the TBE
 4 ε_b on the straight line can be derived:

$$5 \quad \varepsilon_b = \sin\theta \sqrt{\frac{2bv\cos\theta}{k_a k_p}} - \frac{v\sin\theta\cos\theta}{k_a k_p} [1 - \exp\left(-\sqrt{\frac{2bk_a k_p}{v\cos\theta}}\right)] \quad (7)$$

6 where θ is the angle of the straight line to X-axis that is negatively engaged, v is the federate, and $k_a k_p$ is the
 7 open-loop position gain.

8 When circular profiles are machined, TBE occurs at the quadrant transitions as shown in Fig. 13 (b). The
 9 amplitude of the TBE ε_b can be derived:

$$10 \quad \varepsilon_b = R[\sqrt{\cos^2(\phi) + \cos^2(\phi)\sin^2(\omega T)} - \cos(\phi)] \quad (8)$$

11 where R is the designed radius; ω is the angular velocity; ϕ is the phase shift of the feed drive system which
 12 is a function of ω , given by $\phi(\omega) = -\arctan(\frac{\omega}{k_a k_p})$; and the delay time T is given by

$$13 \quad T = \text{real}\left\{\frac{1}{k_a k_p} \left[\frac{(1-i\sqrt{3})C}{6} + \frac{3(1+i\sqrt{3})}{2C} - 1 \right]\right\} \quad (9)$$

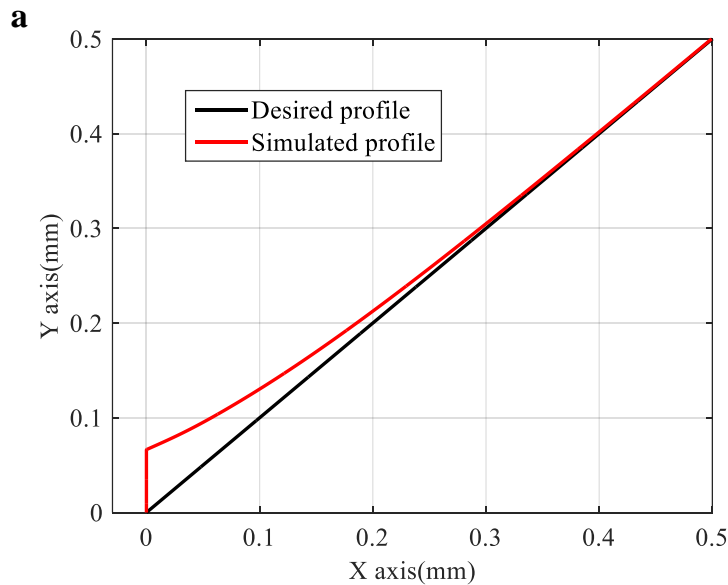
14 where

$$15 \quad C = \sqrt[3]{\frac{\Delta + \sqrt{\Delta^2 - 2916}}{2}} \quad (10)$$

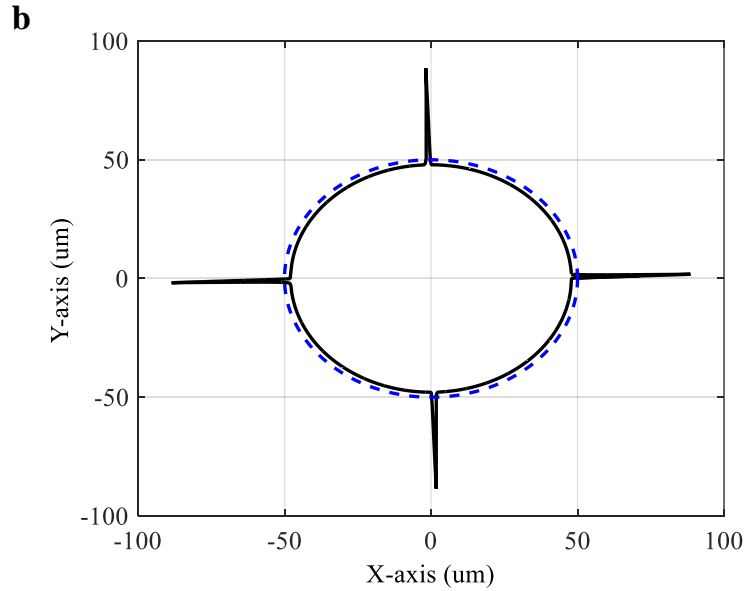
16 with

$$17 \quad \Delta = 54 - 162k_a k_p b \sqrt{\frac{(k_a k_p)^2 + \omega^2}{R\omega^2}} \quad (11)$$

18



1



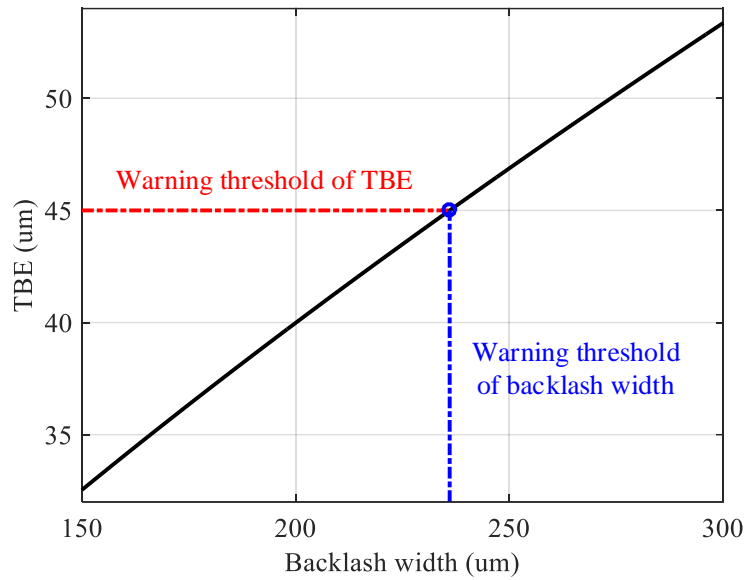
2 Fig. 13 The transient backlash error (a) on a straight line and (b) on a circular profile

3 Thus, Eqs. (7) and (8) fully define the mapping relation between the backlash width b and the TBE ε_b in
 4 the full-closed-loop CNC machine tools respectively in cases of a line and a circle. For further information on
 5 the mechanism of the TBE, please refer to [16].

6 From Eqs. (7) and (8), it can be found that the TBE ε_b is determined by not only the backlash width b , but
 7 also the machining parameters (including the type of the profiles, radius of circle, orientation of straight line,
 8 feedrate, and so on). This implies that in order to calculate the TBE uniquely, the machining parameters should
 9 be specified in advance.

10 Here, we assume such a machining task to be finished: a circular workpiece with radius of 200 mm is to be
 11 milled by the XY contouring system; the open-loop position gains of both axes $k_a k_p$ are equal to 10; and the
 12 feedrate is 200 mm/min. Under such assumption, the one-to-one relationship between backlash width b and
 13 the TBE ε_b can be derived according to Eq. (8), as exhibited by the solid black line in Fig. 14.

1



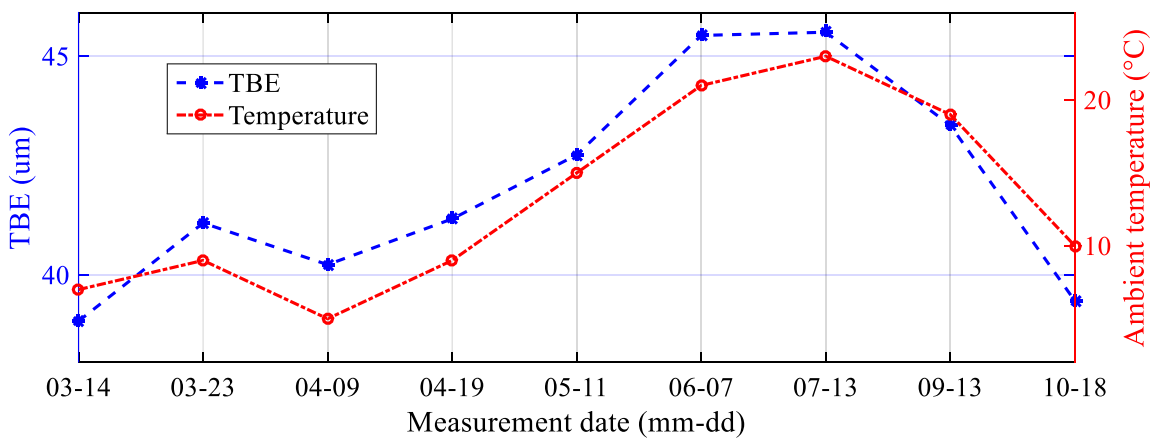
2 Fig. 14 The TBE ϵ_b vs. the backlash width b when machining a circle with a radius of 200 mm at 200
3 mm/min and their warning thresholds

4 **5. The TBE-based maintenance**

5 **5.1 The estimated TBE**

6 In Section 3.2, the backlash widths in Y-axis were tracked and exhibited in Fig. 10. In Section 4.2, the one-
7 to-one relationship between the backlash width b and the TBE ϵ_b is derived and shown in Fig. 14. Based on
8 these foundations, the TBE, caused by the backlash in Y-axis, can be indirectly estimated ultimately, as
9 displayed in Fig. 15.

10



11 Fig. 15 The TBE ϵ_b caused by the backlash width in Y-axis

1 **5.2 The warning threshold of TBE**

2 As shown in Fig. 2, in the TBE-based maintenance system, apart from the real-time TBE should be
3 monitored as the feedback of the maintenance system, the permissible machining error is also needed to be as
4 the input of the maintenance system (namely the warning threshold of the TBE).

5 In general, the permissible machining error is determined by the user-specified tolerance of the workpiece.
6 In our example, it can be assumed that the contour error (roundness error) of the circular workpiece should be
7 smaller than 45 μm . This implies that the warning threshold of TBE equals 45 μm , as shown by the red dash-
8 dot line in Fig. 14.

9 **5.3 Implementation of the TBE-based maintenance**

10 Up to now, the TBE as well as its warning threshold have been obtained respectively in Sections 5.1 and
11 5.2. Therefore, when the monitored TBE ε_b exceeds its warning threshold 45 μm , the maintenance system
12 will notify the maintenance workers to lessen the backlash width.

13 According to the one-to-one mapping relationship between the backlash width and the TBE as indicated by
14 the solid black line in Fig. 14, the permissible maximal size for the backlash can also be quantitatively deduced
15 to be 236.0 μm as indicated by the blue dash-dot line in Fig. 14. So, the value of 236.0 μm can be considered
16 as the warning threshold for the backlash width.

17 The backlash width can be lessened by reloading the ball-screw-nut assembly, reassembling the gearbox,
18 or replacing the mechanical chain.

19 From Fig. 15, it can be observed that in June 7th and July 13th, the monitored TBE were respectively
20 45.48 μm and 45.55 μm , larger than the permissible roundness error 45 μm . Therefore, for ensuring the
21 quality of the produced workpiece, the backlash in the mechanical chain should be lessened to stay within the
22 permissible size.

23 From Fig. 10, it can be found that the mean backlash width \bar{b} in June 7th and July 13th were respectively
24 239.5 μm and 240.1 μm , larger than the warning threshold of the backlash width 236.0 μm . Hence, an
25 identical maintenance decision can be obtained: the mechanical chain should be restored to make its backlash
26 width smaller than 236.0 μm .

27 In this way, the TBE-based maintenance system is finally established, where the real-time TBE is indirectly
28 estimated as the feedback of the maintenance system and the warning threshold of the TBE is customized
29 according to the permissible roundness error as the input. To realize the indirect estimation of the TBE, the

1 width of the backlash in the mechanical chain is measured by utilizing the built-in encoders and the mapping
2 relationship between the backlash width and the TBE was proposed in [16]. When the monitored TBE exceeds
3 its warning threshold, maintenance workers will be notified to lessen the backlash width, and meanwhile, the
4 permissible maximal size for the backlash will also be computed and informed.

5 It should be noticed that before constructing the TBE-based maintenance system, an investigation has been
6 carried out to prove that the TBE is crucial, which deserves to be monitored and controlled.

7 Compared with the CBM proposed in [10], the newly developed TBE-based maintenance system has the
8 following advantages.

9 (1) The TBE is monitored and controlled in a closed loop, and therefore, the quality of the produced
10 workpiece can be ensured.

11 (2) The maintenance action is triggered properly at the occurrence of the excessive machining error, and
12 therefore, premature repairs can be avoided and the maintenance cost can be minimized.

13 (3) Since the mechanism of the TBE has been thoroughly investigated, the maintenance actions can be
14 precisely implemented: first, to lessen the backlash in the mechanical chain; and second, the permissible
15 maximal size for the backlash could be quantitatively worked out.

16 (4) Apart from the built-in encoders, no extra sensor is required, and therefore, the cost for constructing the
17 TBE-based maintenance system can be quite low.

18 **6. Conclusions**

19 (1) To overcome the drawbacks of the conventional CBM, this paper put forward the concept of the MEBM,
20 where the maintenance actions are initiated based on the machining errors rather than the heuristic symptoms.
21 In the MEBM, repairs can be taken properly at the occurrence of the excessive machining errors, and therefore,
22 the premature and redundant maintenance can be avoided and the maintenance cost can be minimized; what's
23 more, the machining errors are controlled in the closed loops, and therefore, the machining accuracy can be
24 guaranteed.

25 (2) Based on the concept of MEBM, the TBE-based maintenance system was established. To achieve this
26 aim, first, encoder-based approaches were developed for specifying the accuracy of the mechanical chain,
27 which is available for the full-closed-loop feed drives. Thereafter, the mechanical chain accuracy was tracked
28 through long-term experiments, showing that compared with the travel variations v_u , v_{300} , and $v_{2\pi}$, the actual

1 mean travel deviation e_p and the backlash width b fluctuate more significantly over time. Besides, the
2 correlation analysis revealed that the changes of e_p and b mainly resulted from the ambient temperature
3 variations.

4 (3) Then, the manufacturing errors, in the full-closed loop CNC machine tools, caused by the mechanical
5 chain inaccuracy are discussed, proving that the TBE is the most crucial error and worth monitoring and
6 controlling. Subsequently, the analytical mapping relationship between the backlash width and the TBE is
7 derived/reviewed.

8 (4) Based on the measured backlash width and its mapping relationship with the TBE respectively obtained
9 in Conclusions (2) and (3), the real-time TBE could be indirectly estimated. The warning threshold of TBE
10 was customized according to the permissible roundness error of the workpiece. Thus, when the monitored TBE
11 exceeds its warning threshold, the maintenance workers would be notified to lessen the backlash width, and
12 meanwhile, the permissible maximal size for the backlash could also be computed and informed. Hence, the
13 TBE-based maintenance system was fully completed, which is capable of controlling the TBE with minimal
14 maintenance cost.

15 **Acknowledgments:**

16 This research is supported by the National Natural Science Foundation of China (Grant nos. 51405373 and
17 51421004), which are highly appreciated by the authors. The authors wish to acknowledge Prof. Gang Jin at
18 South China University of Technology for his comments and suggestions that improved this work.

19 **7. References**

- 20 [1] Nowlan FS, Heap HF (1978) Reliability-centered maintenance. United Airlines, San Francisco,
21 California
- 22 [2] Roy R, Stark R, Tracht K, Takata S, Mori M (2016) Continuous maintenance and the future—Foundations
23 and technological challenges. *CIRP Annals-Manufacturing Technology* 65(2):667-688
- 24 [3] Barlow R, Hunter L (1960) Optimum preventive maintenance policies. *Operations Research* 8(1):90-100
- 25 [4] Lee S, Ni J (2013) Joint decision making for maintenance and production scheduling of production
26 systems. *The International Journal of Advanced Manufacturing Technology* 66:1135-1146
- 27 [5] Tsang AHC (1995) Condition-based maintenance: tools and decision making. *Journal of Quality in*

- 1 Maintenance Engineering 1(3):3-17
- 2 [6] Waeyenbergh G, Pintelon L (2002) A framework for maintenance concept development. International
3 Journal of Production Economics 77(3):299-313
- 4 [7] Dekker R (1996) Applications of maintenance optimization models: a review and analysis. Reliability
5 Engineering & System Safety 51(3):229-240
- 6 [8] Wang H (2002) A survey of maintenance policies of deteriorating systems. European Journal of
7 Operational Research 139(3):469-489
- 8 [9] Jardine AKS, Lin D, Banjevic D (2006) A review on machinery diagnostics and prognostics
9 implementing condition-based maintenance. Mechanical Systems and Signal Processing 20:1483-1510
- 10 [10] Tsai PC, Cheng CC, Hwang YC (2014) Ball screw preload loss detection using ball pass frequency.
11 Mechanical Systems and Signal Processing 48(1):77-91
- 12 [11] Verl A, Heisel U, Walther M, Maier D (2009) Sensorless automated condition monitoring for the control
13 of the predictive maintenance of machine tools. CIRP Annals-Manufacturing Technology 58(1):375-378
- 14 [12] Park C, Moon D, Do N, Bae SM (2016) A predictive maintenance approach based on real-time internal
15 parameter monitoring. The International Journal of Advanced Manufacturing Technology 85:623-632.
- 16 [13] Hoshi T (2006) Damage monitoring of ball bearing. CIRP Annals-Manufacturing Technology 55(1):427-
17 430
- 18 [14] Saravanan S, Yadava GS, Rao PV (2006) Condition monitoring studies on spindle bearing of a lathe. The
19 International Journal of Advanced Manufacturing Technology 28:993-1005
- 20 [15] Takata S, Kimura F, van Houten FJAM, Westkamper E, Shpitalni M, Ceglarek D, Lee J (2004)
21 Maintenance: Changing Role in Life Cycle Management. CIRP Annals - Manufacturing Technology
22 53(2):643-655
- 23 [16] Shi S, Lin J, Wang X, Xu X (2015) Analysis of the transient backlash error in CNC machine tools with
24 closed loops. International Journal of Machine Tools and Manufacture 93:49-60
- 25 [17] Lin J, Qu L (2000) Feature Extraction Based on Morlet Wavelet and Its Application for Mechanical Fault
26 Diagnosis. Journal of Sound and Vibration 234:135-148
- 27 [18] Randall RB, Antoni J (2011) Rolling element bearing diagnostics—A tutorial. Mechanical Systems &
28 Signal Processing 25:485-520
- 29 [19] ISO 230-7:2006. Test Code for Machine Tools - Part 7: Geometric Accuracy of Axes of Rotation

- 1 [20] Shi S, Lin J, Wang X, Zhao M (2016) A hybrid three-probe method for measuring the roundness error
- 2 and the spindle error. Precision Engineering 45:403-413
- 3 [21] ISO 3408-3:2006. Ball Screws – Part 3: Acceptance Conditions and Acceptance Tests